Thermal degradation and flammability of polyamide 11 filled with nanoboehmite

Laurent Ferry, Rodolphe Sonnier, José-Marie Lopez-Cuesta, Sylvain Petigny, Christophe Bert

Thermal degradation and flammability of polyamide 11 filled with nanoboehmite

Laurent Ferry[1] · **Rodolphe Sonnier**[1] · **José-Marie Lopez-Cuesta**[1] · **Sylvain Petigny**[2] · **Christophe Bert**[2]

Abstract The flame-retardant effect of rod-like nanoboehmite was evaluated in biobased polyamide 11. Thermal analysis reveals that hydrated nanofillers modify the degradation pathway of polyamide 11 turning from a two-step to a single-step mechanism. The polymer thermal stability is increased due to interactions between polar groups and filler surface hydroxyl groups. Despite this improved thermal stability, polyamide 11/nanoboehmite composites exhibit shorter times to ignition in cone calorimeter. The phenomenon was attributed to changes in thermoradiative properties leading to a faster heating of the polymer surface. The most significant flame-retardant action is a reduction in heat release rate that was related to a barrier effect while endothermic water release seems to play a minor role.

Keywords Polyamide 11 · Nanoboehmite · Thermal degradation · Flammability · Flame retardant

Introduction

Polyamide 11 (PA11) is a polymer usually used in high-performance applications such as automotive, oil and gas transport, electrical and electronic devices. Produced from castor oil, this polymer is made from renewable resources. However known and produced for several decades, PA11 is gaining interest due to ecological challenges. However, to meet specifications bound to applications, some of the polymer properties have to be improved. Thermal stability and flammability are of primary importance in many areas, such as building, transportation and electrical devices. Only few papers deal with the thermal and fire behavior of PA11.

In 1989, Mailhoslefievre et al. [1] studied the flame retardancy of PA11 using a decabromodiphenyl–antimony trioxide mixture highlighting a bromine–nitrogen synergism. Few years later, Levchik et al. [2] investigated the effect of ammonium polyphosphate (APP) on the thermal decomposition of PA11 and PA12. It was demonstrated that APP modifies their thermal degradation process. The interaction of APP with PA11 implies the formation of intermediate phosphate ester bonds which further decompose to favor the formation of an intumescent char. More recently, Lao et al. [3, 4] used different types of nanoparticles, i.e., silica, clay and carbon fiber, to improve the fire behavior of PA11. Their study showed that nanoparticles enhance the thermal stability of the polymer. However, low amounts of nanoparticles are generally not able to match by themselves the efficiency of current FR additives. Combining nanoclay or carbon nanofiber with an intumescent FR enabled to pass the UL94 V0 rating; however, a minimum of 20 mass% of FR system was required. It is of interest to note that PA11 was also used by Liu et al. [5] in an intumescent flame-retardant system to play the role of a macromolecular charring agent. PA11 was chosen to improve the compatibility between the FR system and the host polymer (polypropylene). Although PA11 is intrinsically a poor char former [6], a synergistic effect was observed between polyamide and pentaerythritol giving rise to an increase in char amount.

✉ Laurent Ferry
laurent.ferry@mines-ales.frl

[1] Centre des Matériaux des Mines d'Alès C2MA, Ecole des Mines d'Alès, 6 Avenue de Clavières, 30319 Alès Cedex, France

[2] Saint-Gobain, CREE, 550 Avenue Alfred Jauffret, BP 224, 84306 Cavaillon Cedex, France

The use of hydrated mineral fillers is a common and efficient way to improve the fire behavior of polymers [7]. Moreover, mineral particles can be considered as a low environmental impact flame-retardant solution particularly adapted to biobased polymers. Magnesium hydroxide has already been used in several polyamides [8, 9]. It was shown that the effect of the hydrated filler depends on its decomposition temperature relative to that of the host polymer. Anyway, high filler contents are required to fulfill fire standards. Boehmite is another hydrated filler acting as flame retardant which is relatively less used that magnesium hydroxide or aluminum trihydroxide due to a lower endothermic effect but which decomposes at higher temperature avoiding processing difficulties [10]. Microsized boehmite was also used in synergy with phosphorus and nitrogen flame retardant in epoxy resins [11, 12]. Few years ago, boehmite was obtained as nanofiller under different morphologies by Saint-Gobain: rods, platelets, spheres [13]. More recently, Elbasuney reported a novel continuous flow manufacture of boehmite nanorods by hydrothermal synthesis [14]. The thermal stability of boehmite nanofibers was shown to depend on the hydrothermal conditions of synthesis and therefore on their diameter [15]. Similarly to microsized boehmite, nanoboehmite can also act synergistic agent in complex flame-retardant system [16–18]. Only few papers deal with the use of nanoboehmite as unique filler to modify the fire behavior of polymers [19–22]. To the best of our knowledge, no work was reported about nanoboehmite into PA11.

In this work, the thermal stability and the flammability of PA11 filled with rod-like nanoboehmite were investigated. The aim of the study was to elucidate the physical and chemical modes of action of nanoboehmite during PA11 combustion.

Experimental

Materials

Polyamide 11 Rilsan® BMNO TLD grade was kindly supplied by Arkema. The melting point was 189 °C and the specific gravity 1.03 g cm^{-3}.

Rod-like boehmite nanofillers CAM 9010 with a specific surface area of about 130 m^2 g^{-1} were obtained from Saint-Gobain CREE (Cavaillon, France). The nanoparticles had a length around 150 nm and a diameter around 20 nm.

Nanocomposites were melt blended using Haake Rheomix 3000 batch mixer at 230 °C (screw speed = 180 rpm, mixing time). Before processing, the polymer was dried at 80 °C for 4 h. 100 × 100 × 4 mm^3 plates were prepared by injection molding at 230 °C using a Krauss Maffei KM 50t machine. CAM9010 was incorporated at two different loadings in PA11, respectively, 10 and 30 mass%. These loadings may be considered as high for nanocomposites. However, they were chosen based on results from the literature. Thus, Sun et al. [22] and Laachachi et al. [19] used lamellar nanoboehmite up to, respectively, 10 and 20 mass%. These contents were necessary to obtain significant change in thermal and flammability properties.

Instrumentation

A scanning electron microscope (FEI 110 Quanta 200 SEM) was used to study the morphology of the samples. All images were obtained under high vacuum at a voltage of 10.0 kV with a spot size of 2.5 and a working distance of 8 mm. Scanning transmission electron microscopy (STEM) measurements were performed using a TEM Jeol 1200EX2. The STEM cross-sectional samples were prepared with a cryo-ultramicrotome. The thickness of these samples varied in the range of 60–100 nm.

The thermal decomposition was investigated using a PerkinElmer Pyris-1 TGA. All measurements were performed under nitrogen with a heating rate of 10 °C min^{-1}. The sample mass was 8 ± 2 mg. The TG instrument was coupled to an FTIR spectrometer (Bruker-IFS66) to analyze the evolved gases. The heating rate and sample mass were identical to those of a simple TG run (10 °C min^{-1} and 8 mg). The evolved gases were transferred into the FTIR spectrometer via a heated line (at 200 °C) with a nitrogen flow rate of 20 mL min^{-1}. FTIR spectra were obtained by averaging eight scans and recorded in the region 400–4000 cm^{-1} with a spectral resolution of 1 cm^{-1}.

Evaluation of the flammability properties was made using a Pyrolysis Combustion Flow Calorimeter (PCFC) from Fire Testing Technology (FTT). In PCFC tests, the samples, whose mass is 2 ± 0.5 mg, are heated from 20 to 900 °C at various heating rates (1, 2 and 3 K s^{-1}) in a pyrolyzer. The degradation products are transported by an inert flux and then mixed with oxygen when entering a combustor at 900 °C where the decomposition products are completely burnt. The heat release rate (*HRR*) is measured as function of temperature. In order to compare materials, the heat release capacity, *HRC* (J g^{-1} K^{-1}), is usually determined. *HRC* refers to the ratio of peak of HRR (*pHRR*) upon heating rate. In our case, the decomposition of samples involved several steps. Therefore, *sumHRC* was used rather than HRC. *SumHRC* is the sum of HRC values of every decomposition peak after deconvolution performed with the FTT software. The measurement uncertainty for PCFC data is considered to be 5%.

Fire properties were assessed using a FTT cone calorimeter. Tests were carried out on 100 × 100 × 4 mm^3 specimens using incident heat fluxes of 35, 50 and 65 kW m^{-2}, in accordance with the ISO 5660 standard.

Ignition time, total heat release (*THR*) and peak of heat release rate (*pHRR*) were obtained as main data. The measurement uncertainty for cone calorimeter data is considered to be 10%.

Fire behavior characterization was completed by an epiradiator test inspired from AFNOR NF P 92-505. The samples with 70 × 70 × 4 mm^3 dimensions were placed on a metallic grid at 30 mm of a heat source of 500 W, corresponding to a heat flux of 37 kW m^{-2}. The temperature of the upper surface of the specimen as function of time was recorded using an infrared pyrometer Optris CT. In order to perform the temperature measurement, the epiradiator was removed and replaced within a short period of time (1 s). Time to ignition was also measured.

Thermal diffusivity was measured using a Linseis XFA 600 Xenon Flash Apparatus at room temperature on 1-mm-thick sample coated with graphite on both surfaces. The measurement uncertainty was around 5%.

Results and discussion

Microstructure

PA11/boehmite nanocomposites have been observed by scanning transmission electron microscopy (STEM). Figure 1a reveals that, at 10 mass% content, nanoboehmite is well dispersed in the polyamide matrix. As a matter of fact, individual rod-like particles may be observed with length consistent with the one announced by the supplier (circa 150 nm). At a higher content (30 mass%), the nanofillers are still relatively well dispersed even though some submicronic aggregates could be seen (Fig. 1b).

TG-FTIR coupling

Thermal stability of virgin PA11 and PA11 filled with 10 and 30 mass% of CAM9010 was investigated by TG under nitrogen atmosphere. As shown in Fig. 2, PA11 degrades in two steps between 350 and 500 °C similarly to other polyamides [23]. The main step is located around 430 °C, whereas the second and minor step occurs over 450 °C. At high temperature, PA11 does not form any charred residue.

In the presence of nanoboehmite, the thermal stability of PA11 is increased. The decomposition occurs in a single step shifted toward high temperature by 30 °C compared to pure PA11, whatever the filler content. The difference between TG curves of pure and filled polymer cannot be described by a simple rule of mixtures between PA11 and CAM9010 since nanoboehmite decomposition results only in a 15% mass loss occurring between 450 and 500 °C. Therefore, TG curves of filled PA11 indicate a change in the degradation pathway. The residue amounts correspond exactly to the nanoboehmite content after water release (15 mass% of nanoparticle mass). Thus, it can be concluded that nanoboehmites do not favor polymer charring.

Degradation products have been analyzed by TG-FTIR coupling. In virgin PA11, the main absorption bands correspond to vibrations of CH_2 (2800–3000 cm^{-1}), C=O (1700 cm^{-1}) and N–H (1470 cm^{-1}). These different peaks have been integrated (Gram–Schmidt curves) in order to follow the evolution of their intensity as a function of temperature.

Figure 3 reveals that the first step of PA11 degradation, located around 440 °C, generates gaseous species containing C=O, N–H and CH_2 groups. Levchik et al. [6] in their review on thermal decomposition of aliphatic polyamides indicate that the degradation of PA11 under inert atmosphere produces mainly lactams, nitriles and unsaturated hydrocarbons. It may be assumed that these decomposition products are released in this range of temperature. During the second step of decomposition around 475 °C, the degradation products are mainly constituted by hydrocarbons as highlighted by the peak of the CH_2 Gram–Schmidt. This may be ascribed to the decomposition of a non-stable char formed from the unsaturated hydrocarbon oligomers after the first decomposition step of PA11.

The same analysis was performed on PA11-10%CAM9010 composite (Fig. 3b). This time, the Gram–

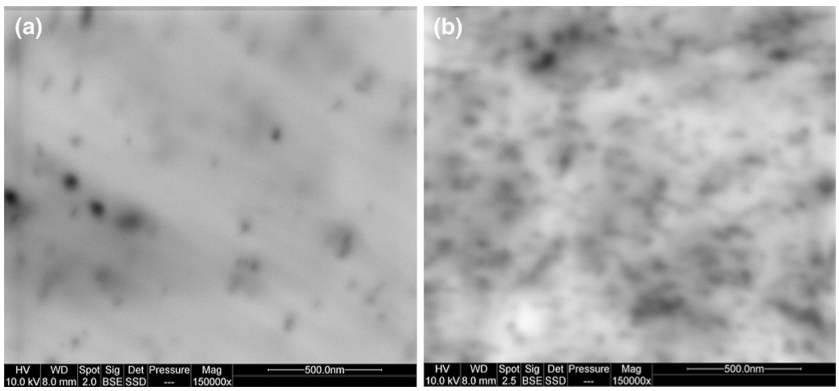

Fig. 1 STEM images of PA11/boehmite nanocomposite
a PA11 + 10%CAM9010,
b PA11 + 30%CAM9010

Schmidt curves of the C=O, N–H and CH_2 absorption bands exhibit exactly the same behavior. The higher evolved gases production is observed at 480 °C. Similar results have been obtained with the PA11-30%CAM9010 composite. This means that CAM9010 is likely to change the degradation pathway of PA11. The decomposition products containing amine and carboxyl groups are released at higher temperature.

Considering TG-FTIR coupling results, it may be assumed that nanoboehmite increases the thermal stability of PA11 due to interactions between surface hydroxyl groups of the hydrated filler and polar groups of the polymer matrix, i.e., NH and C=O groups. Interactions are supposed to be hydrogen bonds inducing a significant shift of degradation onset of about 30 °C. The fact that NH and C=O containing species are released at higher temperature and simultaneously with hydrocarbons implies that no intermediary char is formed. This result will be of particular interest for bench scale test (see "Cone calorimeter" section).

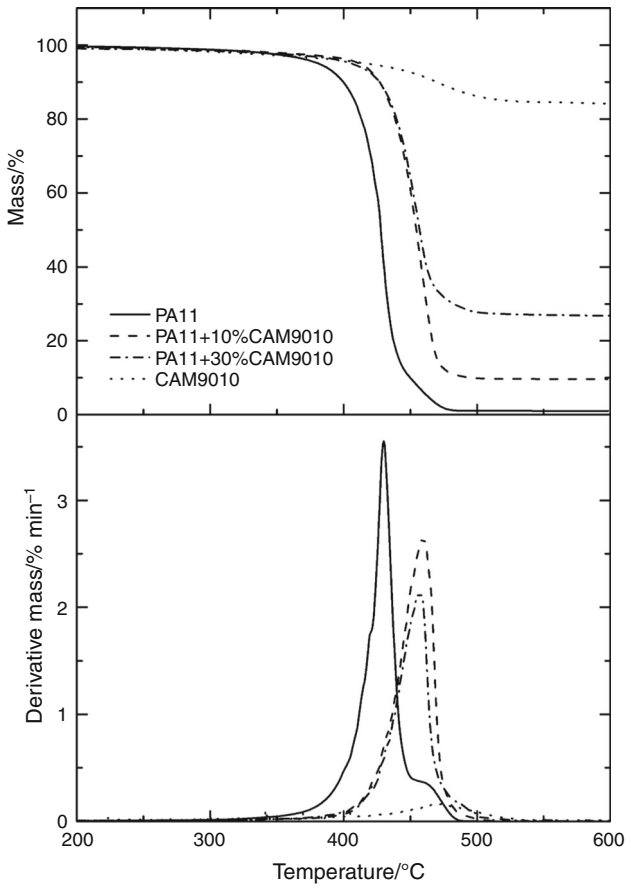

Fig. 2 TG (**a**) and DTG (**b**) curves of pure and filled PA11 under nitrogen

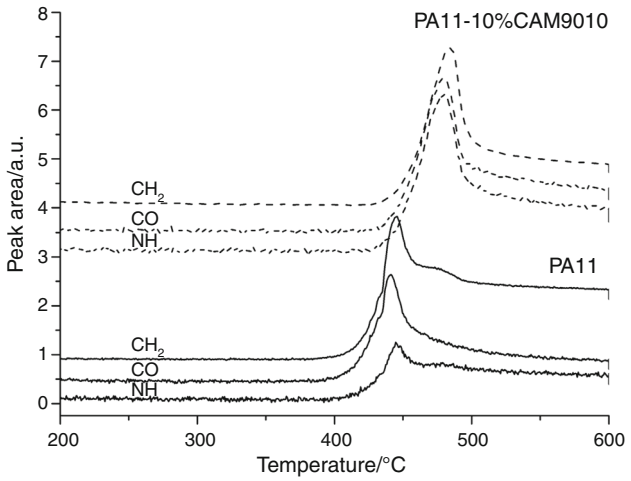

Fig. 3 Gram–Schmidt of CH_2, C=O and N–H bands as a function of temperature for pure PA11 (*solid lines*) and PA11 + 10%CAM9010 (*dashed lines*)

PCFC

Similar to what was observed by TG, PCFC curve shows that PA11 degrades in two steps (Fig. 4) at 430 and 475 °C, respectively. The presence of nanoboehmite induces a shift of heat release rate peak to high temperature. The degradation temperature is significantly increased whatever the filler content.

Table 1 shows that the total heat release (*THR*) decreases proportionally to nanoboehmite content ($THR = -0.3029 \times \text{CAM9010 content} + 32.671$ with $R^2 = 0.9999$) what reveals a simple dilution effect of fuel in the condensed phase. The evolution of heat release capacity (*HRC*), defined as the ratio of main peak of heat release rate (*pHRR*) over the heating rate, does not observe a similar linear decrease. This may be attributed to the two-step decomposition of pure PA11. From the assumption that virgin PA11 curve results from the convolution

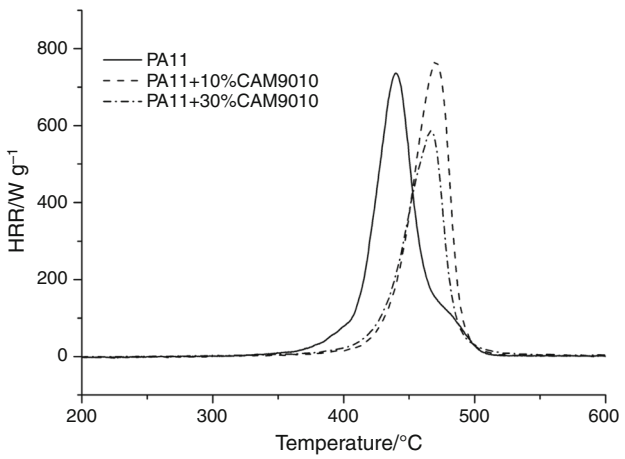

Fig. 4 HRR versus temperature for pure and filled PA11 (heating rate = 1 K s^{-1})

Table 1 Energy and mass parameters determined from TG and PCFC tests

CAM9010 content (%)	*THR*/kJ g^{-1}	Mass loss/%	EHC_T/kJ g^{-1}	*HRC*/J g^{-1} K^{-1}	*sumHRC*/J g^{-1} K^{-1}	*MLC*/% K^{-1}	EHC_P/kJ g^{-1}
0	32.7	99	33	736	847	3.61	20.4
10	29.6	90	32.9	768	768	2.47	31.1
30	23.6	73.5	32.1	587	587	2.03	28.9

between two degradation peaks, the sum of both *HRC* can be calculated. Replacing *HRC* by *sumHRC* leads to a linear decrease with filler content ($sumHRC = -8.7214 \times$ content $+ 850.29$ with $R^2 = 0.9989$). Hence, the dilution effect is confirmed.

The comparison of TG and PCFC brings useful information about the effective heat of combustion (*EHC*) of degradation products which is defined as the heat released by gram of evolved gases. Since both tests were not performed using the same heating rate, *EHC* cannot be estimated at every temperature. However, *EHC* can be calculated considering the whole experiment by dividing *THR* by mass loss (EHC_T). Table 1 indicates that EHC_T are almost similar whatever the composition. The presence of nanoboehmite should normally reduce EHC_T due to the water release. Nevertheless, the amount of water (15 mass% of nanoboehmite) seems too low to induce a significant effect.

EHC can also be assessed at the maximum of degradation assuming that the heating rate does not affect the degradation pathway of PA11. In this case, EHC_P is obtained by dividing *HRC* by the mass loss capacity (*MLC*). *MLC* can be defined as the peak of mass loss rate (*pMLR*) divided by the heating rate. EHC_P of PA11/nanoboehmite composites are similar to those obtained considering the whole experiment, whereas the value for pure PA11 is relatively lower. It must be reminded that PA11 degradation is a two-step mechanism; therefore, the decomposition products evolved during the main step are likely to be those exhibiting the lower heat release when burning, i.e., NH and C=O containing species.

Kinetic study

To go further with the influence of nanoboehmite on the PA11 thermal degradation, a kinetic study was performed. Tests were carried out using PCFC at three different heating rates (1, 2 and 3 K s^{-1}).

Generally, the degradation rate is described by the basic rate equation [24] (Eq. 1):

$$\frac{d\alpha}{dt} = A \exp(-E_a/RT) f(\alpha) \quad (1)$$

where α is the conversion fraction, E_a is the activation energy of the reaction, A the pre-exponential factor and $f(\alpha)$ a function depending on the reaction model to be used (zero order, first order, etc.).

Assuming a first-order reaction, the Kissinger equation was used (Eq. 2).

$$\ln\left(\frac{\beta}{T_m^2}\right) = \ln\left(\frac{A}{E_a}\right) - \frac{E_a}{RT_m} \quad (2)$$

Here, β is the heating rate (K s^{-1}), T_m is the maximum degradation rate temperature (K). Thus, E_a and A can be determined from the linear dependence of $\ln(\beta/T_m^2)$ versus $1/T_m$ plot for various heating rates.

This method was applied to PCFC curves after deconvolution (Fig. 5). PA11 decomposition was assumed to be a two-step mechanism, each step being described by a gaussian function. Fitting experimental results with the gaussian law enables to determine T_m^1 and T_m^2 corresponding to the maximum degradation rate of each step. The same method was used for nanoboehmite filled PA11 even though decomposition seems to turn from a two-step to a single-step mechanism.

Table 2 shows the values of activation energy E_a and pre-exponential factor A for both degradation steps. The results indicate that the presence of nanoboehmite increases the activation energy of the first step of decomposition, whereas it decreases the activation energy of the second step. This is consistent with the increase in thermal stability observed by TG. To sum up, the presence of nanoboehmite tends to merge both degradation steps in a single one occurring at intermediate temperature.

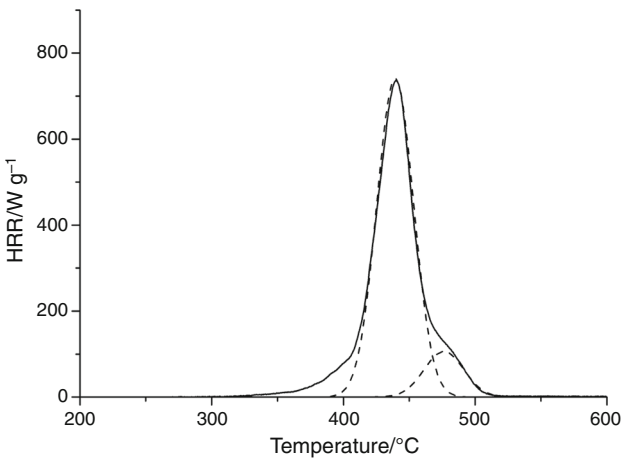

Fig. 5 Example of deconvolution in the case of PA11 at 1 K s^{-1}

Cone calorimeter

With the aim to assess the fire behavior, cone calorimeter tests have been performed on pure PA11 and 10 and 30 mass% nanoboehmite filled PA11. Three different irradiances 35, 50 and 65 kW m^{-2} were used. Examples of *HRR* are presented in Fig. 6. The corresponding data are gathered in Table 3.

Two important facts should be underlined: (1) the presence of nanoboehmite reduces the time to ignition (*TTI*) of PA11; this effect is particularly enhanced when the irradiance decreases and seems contradictory to the improved thermal stability observed by TG or PCFC. (2) *pHRR* of PA11 is slightly affected at low boehmite content (10%), whereas a significant decrease is observed at higher content (30%). The *pHRR* decrease is all the greater that irradiance is low. It should be remarked that after ignition *HRR* increases, rapidly stabilizes and then slowly decreases for an important period of time. This behavior is typical of the formation of a protective layer at the surface of the sample that controls the heat and mass transfer and thus the pyrolysis rate.

From Tables 1 and 3, it can be remarked that *HRC* and *pHRR* follow the same trend. There is a qualitative agreement between PCFC and cone calorimeter. The 10% nanoboehmite composition behaves very similar to pure PA11, whereas the 30% nanofiller composition exhibits significantly lower *HRR* peaks.

As it was proposed in a previous paper [25], a very interesting representation consists in plotting the normalized *HRC* designated as *R1* versus the normalized *pHRR* designated as *R2*. $R1 = HRCcomposite/HRCmatrix$ and $R2 = pHRRcomposite/pHRRmatrix$. A mismatch to the $R1 = R2$ line indicates that reduced flammability implies physical effects, and particularly barrier effect, whereas PCFC measurements enable essentially to evidence chemical effects. Figure 7 reveals a strong mismatch to $R1 = R2$; thus, the decrease of *pHRR* in cone calorimeter test may be ascribed to a barrier effect generated at the surface of the sample during combustion. This effect is significant at 30 mass% nanoboehmite content, while it remains inefficient at 10 mass%.

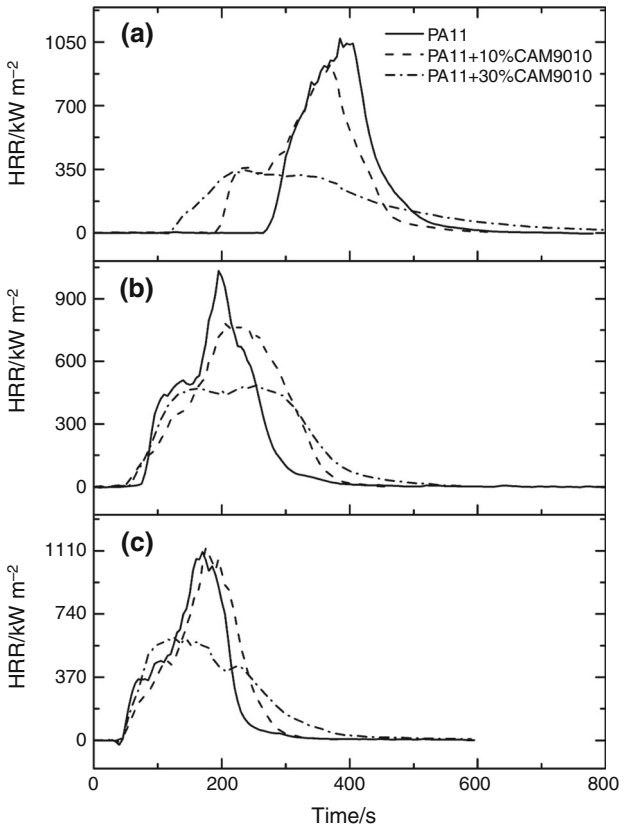

Fig. 6 *HRR* versus time for pure and filled PA11 **a** 35 kW m^{-2} **b** 50 kW m^{-2} **c** 65 kW m^{-2}

According to cone calorimeter data, the effective heat of combustion of gases has been calculated by dividing the *THR* by the mass loss (*ML*). Taking into account that nanoboehmite releases non-combustible water vapor during decomposition, *EHC* has been re-calculated after subtraction of water mass from mass loss (EHC_{mod}). The calculations were performed considering the 50 kW m^{-2} test. Table 3 highlights that EHC_{mod} is slightly higher in the presence of boehmite. These results are not fully consistent with those obtained by PCFC since EHC_T was observed to be independent of boehmite content. However, it should be reminded that in PCFC polymer is pyrolyzed under nitrogen and then degradation products are completely burnt at 900 °C. These conditions differ somewhat

Table 2 Kinetic parameters of each step of decomposition

CAM9010 content (%)	Step 1		Step 2	
	E_a/kJ mol^{-1}	A/s^{-1}	E_a/kJ mol^{-1}	A/s^{-1}
0	92	1.24×10^5	272	1.09×10^{18}
10	116	4.15×10^6	107	7.62×10^5
30	126	2.38×10^7	134	8.19×10^7

Table 3 Cone calorimeter data for pure and filled PA11 (50 kW m^{-2})

CAM9010 content/ %	*TTI*/ s	*pHRR*/ kW m^{-2}	*THR*/ MJ m^{-2}	*EHC*/ kJ g^{-1}	*EHCmod*/ kJ g^{-1}	Residue/ %	Calculated char/ %	CO/CO_2/ mg g^{-1}*
0	83	971	121	31.6	31.6	9.3	9.3	10.9
10	85	963	136	33.5	34.1	11.6	3.1	7.5
30	62	518	123	31.6	33.6	24.8	−0.7	7.9

* The ratio CO/CO_2 was the mean value recorded between 100 and 350 s

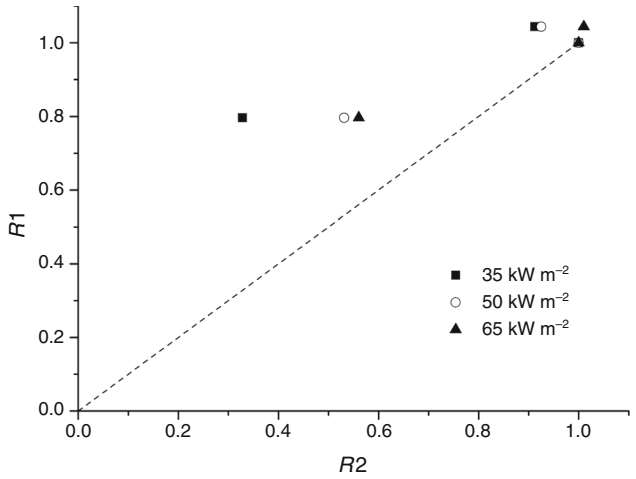

Fig. 7 *R*1 versus *R*2

from those of cone calorimeter where combustion may be incomplete (production of CO instead of CO_2). If combustion is incomplete, the oxygen consumption is reduced, and thus, heat release and *EHC* are decreased. It was observed that the CO/CO_2 ratio during combustion was higher in the case of pure PA11 than in the case of filled PA11. This could be an explanation for the slightly lower *EHC* of pure PA11.

Table 3 also shows the residue amount after cone calorimeter tests at 50 kW m^{-2}. From these data, the fraction of char can be calculated by subtracting the amount of dehydrated boehmite from the residue [Char (%) = Residue (%) – 0.85 × boehmite (%)]. It can be seen that pure PA11 gives a non-negligible amount of char, i.e., 9.3%. This char results from the specific two-step degradation pathway of the pure polymer that leads, after evolution of NH and C=O species, to conjugated unsaturated oligomers which are likely to aromatize. It may be underlined that in the presence of oxygen, PA11 degradation is somewhat different from that under inert atmosphere, leading to the formation of conjugated unsaturated oligoenimines which can favor char [6, 26]. On the contrary, the presence of nanoboehmite strongly reduces and even inhibits the formation of char. This should be related to the change of degradation pathway as evidenced by TG-FTIR experiments. Decomposition of filled PA11 is a single-step mechanism leading to the simultaneous release of all degradation products without forming any char. The decrease of char yield in nanocomposites is consistent with the before-mentioned increase of EHC_{mod} since the fuel load is de facto enhanced.

Photographs of residues of cone calorimeter tests are presented in Fig. 8. In the case of PA11, a thin but cohesive black char layer is formed from the early time of the experiment. This layer traps the decomposition gases up to ignition inducing a blowing of the upper surface. After ignition, the layer deflates since combustible gases are consumed in the flame. At 10 mass% nanoboehmite content, the residue is gray and no more cohesive. At 30 mass% boehmite content, the residue is still gray but becomes cohesive.

These observations are consistent with the before-mentioned phenomena. It appears that there is an antagonist effect of nanoboehmite. On the one hand, nanoboehmite reduces the ability of PA11 to char formation due to a change in the degradation pathway. This effect enhances the polymer *EHC* and may play a role in the lower ignition time. On the other hand, nanoboehmite, after dehydration, forms a protective mineral layer acting as barrier against heat and mass transfer, thus reducing mass loss rate and *pHRR*.

Epiradiator test

In order to highlight the exact role of nanoboehmite on the ignition time, surface temperature evolution was investigated using epiradiator as heating source. Epiradiator was preferred to cone calorimeter because surface temperature can easily be measured without any contact using an infrared pyrometer.

Ignition temperatures are summed up in Table 4. Ignition temperatures are consistent with the thermal stabilities as determined by TG or PCFC. PA11 ignites at relatively lower temperature than the filled polymers. It may be supposed that ignition occurs when a critical flow rate of combustible gases is reached. This allegation is supported by the fact that for the three materials ignition occurs at a temperature corresponding approximately to the same *HRR* of 50 W g^{-1} (see Fig. 4). Table 4 also

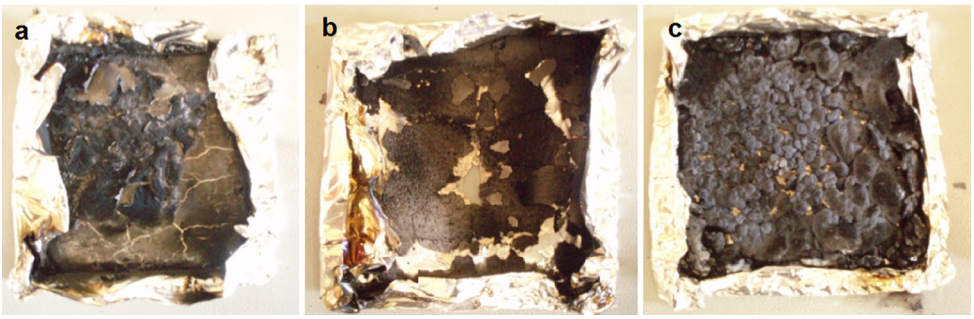

Fig. 8 Photographs of residues after cone calorimeter test at 50 kW m^{-2} **a** PA11 **b** PA11 + 10%CAM9010 **c** PA11 + 30%CAM9010

Table 4 Ignition temperature and time measured during epiradiator test and thermal diffusivity for pure and filled PA11

CAM9010 content/%	Ignition temperature/°C	Ignition time/s	Thermal diffusivity/cm^2 s^{-1}
0	387	60	0.0015
10	433	44	0.0016
30	434	55	0.0021

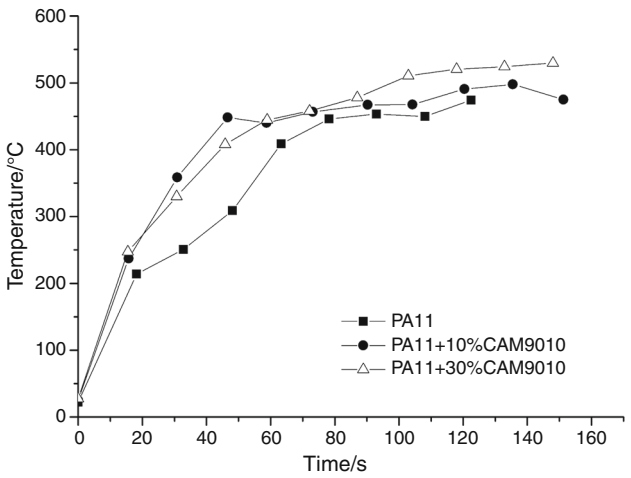

Fig. 9 Experimental surface temperature of samples during epiradiator test

shows that ignition times are consistent with those obtained with cone calorimeter. Nanoboehmite filled PA11, although more thermally stable, exhibit lower ignition time than pure PA11.

Figure 9 shows the evolution of temperature versus time for pure and filled PA11 under a 37 kW m^{-2} irradiance. The results reveal that the heating rate of the upper surface is lower in the case of PA11 compared to filled polymers.

Table 4 shows the values of the thermal diffusivity obtained for pure PA11 and for nanocomposites. It can be noticed that the thermal diffusivity increases when nanofiller is added to the PA11 matrix. Therefore, it can be concluded that the surface of filled PA11 should be heated more slowly than that of pure polymer since heat is transferred more rapidly from the surface to the inner part of the sample. These results enable to highlight a contradiction between experimental and theoretical surface heating rates. Several hypotheses can be proposed to explain the higher surface heating rate in the presence of boehmite: (1) the absence of char layer in the pre-ignition period in comparison with pure PA11, (2) a lower endothermic effect due to the melting of crystalline phase of PA11, (3) a difference of thermoradiative properties (emissivity or in-depth absorptivity). This latter assumption seems the more likely to affect significantly the heating rate. In the presence of nanoboehmite, the incident radiative flux of cone calorimeter (or epiradiator) would be mainly transmitted to the material at the surface due to a higher absorptivity of fillers (especially in the infrared range). In the case of pure PA11, the radiative flux may penetrate more deeply in the material before being absorbed. To conclude, ignition time seems mainly governed by thermoradiative properties of fillers rather than the thermal stability of the material.

Conclusions

The study of PA11-nanoboehmite composites reveals that the presence of nanofillers has a positive effect on fire behavior as well as thermal stability of the polymer by shifting the degradation onset by approximately 30 °C. This effect was related to physical interactions between boehmite surface and polar groups of PA11 changing the degradation pathway of this polymer. This stabilization effect affects directly ignition temperature but not ignition time which is reduced in the presence of boehmite. This latter phenomenon was related to an increase of the surface heating rate in filled polymer due the modification of thermoradiative properties of the material. After ignition, it was highlighted that nanoboehmite improves the fire behavior of PA11 by reducing significantly both the *pHRR* and the mass loss rate. This was ascribed to a barrier effect particularly efficient at low irradiance.

References

1. Mailhos-Lefievre V, Sallet D, Martel B. Thermal degradation of pure and flame-retarded polyamides 11 and 12. Polym Degrad Stab. 1989;23:327–36.
2. Levchik SV, Costa L, Camino G. Effect of the fire-retardant, ammonium polyphosphate on the thermal decomposition of aliphatic polyamides. I. Polyamides 11 and 12. Polym Degrad Stab. 1992;36:31–41.
3. Lao SC, Wu C, Moon TJ, Koo JH, Morgan A, Pilato L, Wissler G. Flame-retardant polyamide 11 and 12 nanocomposites: processing, morphology and mechanical properties. J Compos Mater. 2009;43:1803–18.
4. Lao SC, Koo JH, Moon TJ, Londa M, Ibeh CC, Wissler GE, Pilato LA. Flame-retardant polyamide 11 nanocomposites: further thermal flammability studies. J Fire Sci. 2011;29:479–98.
5. Liu Y, Feng ZQ, Wang Q. The investigation of intumescent flame-retardant polypropylene using a new macromolecular charring agent polyamide 11. Polym Compos. 2009;30:221–5.
6. Levchik SV, Weil ED, Lewin M. Thermal decomposition of aliphatic nylons. Polym Int. 1999;48:532–57.
7. Hornsby PR. Fire-retardant fillers. In: Wilkie CA, Morgan AB, editors. Fire retardancy of polymeric materials. New-York: CRC Press; 2010. p. 163–85.
8. Hornsby PR, Wang J, Rothon R, Jackson G, Wilkinson G, Cossick K. Thermal decomposition behaviour of polyamide fire-retardant compositions containing magnesium hydroxide filler. Polym Degrad Stab. 1996;51:235–49.
9. Fei G, Liu Y, Wang Q. Synergistic effects of novolac-based char former with magnesium hydroxide in flame retardant polyamide-6. Polym Degrad Stab. 2008;93:1351–6.
10. Camino G, Maffezzoli A, Braglia M, De Lazzaro M, Zammarano M. Effect of hydroxides and hydroxycarbonate structure on fire retardant effectiveness and mechanical properties in ethylene-vinyl acetate copolymer. Polym Degrad Stab. 2001;74:457–64.
11. Müller P, Schartel B. Melamine poly(metal phosphates) as flame retardant in epoxy resin: performance, modes of action, and synergy. J Appl Polym Sci. 2016;133:43549–62.
12. Sut A, Greiser S, Jäger C, Schartel B. Synergy in flame-retarded epoxy resin: identification of chemical interactions by solid-state NMR. J Therm Anal Calorim. 2016. doi:10.1007/s10973-016-5934-4.
13. Bravet D, Guiselin O, Swei G. Effect of surface treatment on the properties of polypropylene/nanoboehmite composites. J Appl Polym Sci. 2010;116:373–81.
14. Elbasuney S. Continuous hydrothermal synthesis of AlO(OH) nanorods as a clean flame retardant agent. Particuology. 2015;22:66–71.
15. Xu X, Liu Y, Li Z, Lv Z, Song J, He M, Wang Q, Yan L, Li Z. Thermal study of boehmite nanofibers with controlled particle size. J Therm Anal Calorim. 2014;115:1111–7.
16. Pawloski KH, Schartel B. Flame retardancy mechanisms of aryl phosphates in combination with boehmite in bisphenol A polycarbonate/acrylonitrileebutadieneestyrene blends. Polym Degrad Stab. 2008;93:657–67.
17. Friederich B, Laachachi A, Sonnier R, Ferriol M, Cochez M, Toniazzo V, Ruch D. Comparison of alumina and boehmite in (APP/MPP/metal oxide) ternary systems on the thermal and fire behavior of PMMA. Polym Adv Technol. 2011;23:1369–80.
18. Hamdani-Devarennes S, El Hage R, Dumazert L, Sonnier R, Ferry L, Lopez-Cuesta JM, Bert C. Water-based flame retardant coating using nano-boehmite for expanded polystyrene (EPS) foam. Prog Org Coat. 2016;99:32–46.
19. Laachachi A, Ferriol M, Cochez M, Lopez Cuesta JM, Ruch D. A comparison of the role of boehmite (AlOOH) and alumina (Al_2O_3) in the thermal stability and flammability of poly(methyl methacrylate). Polym Degrad Stab. 2009;94:1373–8.
20. Zhang J, Ji Q, Zhang P, Xia Y, Kong Q. Thermal stability and flame-retardancy mechanism of poly(ethylene terephthalate)/boehmite nanocomposites. Polym Degrad Stab. 2010;95:1211–8.
21. Monti M, Camino G. thermal and combustion behavior of polyethersulfone-boehmite nanocomposites. Polym Degrad Stab. 2013;98:1838–46.
22. Sun T, Zhuo Q, Chen Y, Wu Z. Synthesis of boehmite and its effect on flame retardancy of epoxy resin. High Perform Polym. 2015;27:100–4.
23. Herrera M, Matuschek G, Kettrup A. Main products and kinetics of the thermal degradation of polyamides. Chemosphere. 2001;42:601–7.
24. Budrugeac P, Segal E. Applicability of the Kissinger equation in thermal analysis. J Therm Anal Calorim. 2007;88:703–7.
25. Sonnier R, Ferry L, Longuet C, Laoutid F, Friederich B, Laachachi A, Lopez-Cuesta JM. Combining cone calorimeter and PCFC to determine the mode of action of flame-retardant additives. Polym Adv Technol. 2011;22:1091–9.
26. Oliveira MJ, Botelho G. Degradation of polyamide 11 in rotational moulding. Polym Degrad Stab. 2008;93:139–46.